Neuron
Article

Calcium Store Depletion Induces Persistent Perisomatic Increases in the Functional Density of *h* Channels in Hippocampal Pyramidal Neurons

Rishikesh Narayanan,[1,2] Kevin J. Dougherty,[1] and Daniel Johnston[1,*]
[1]Center for Learning and Memory, The University of Texas at Austin, Austin, TX 78712, USA
[2]Present address: Molecular Biophysics Unit, Indian Institute of Science, Bangalore 560012, India
*Correspondence: djohnston@mail.clm.utexas.edu
DOI 10.1016/j.neuron.2010.11.033

SUMMARY

The regulation of intracellular calcium by the endoplasmic reticulum (ER) plays a critical role in neuronal function. While the consequences associated with depleting calcium from the ER have been studied in multiple systems, it is not known whether the intrinsic properties of a neuron change in response to such perturbations. In this study, we demonstrate that the depletion of calcium from the ER of hippocampal CA1 pyramidal neurons induces a persistent, perisomatic increase in the density of functional *h* channels resulting in a reduction in intrinsic excitability and an increase in the optimal response frequency. This form of intrinsic plasticity is dependent on the elevation of cytoplasmic calcium, inositol triphosphate receptors, store-operated calcium channels, and the protein kinase A pathway. We postulate that this form of depletion-induced intrinsic plasticity is a neuroprotective mechanism that reduces excitability after depletion of calcium stores triggered through altered network activity during pathological conditions.

INTRODUCTION

The endoplasmic reticulum (ER) plays crucial roles in various aspects of neuronal physiology and pathophysiology. The regulation of calcium by the ER is vital for many intra-ER signaling cascades that execute important functions such as cytoplasmic calcium homeostasis, synthesis and maturation of proteins, regulation of gene expression, and integration of intraneuronal information (Berridge, 2002; Mattson et al., 2000; Park et al., 2008; Verkhratsky, 2005). Calcium homeostasis within the ER is an active and delicate process, especially given the steep concentration gradient between ER calcium (μM range) and the cytoplasmic calcium (nM range) levels. This process is controlled by calcium release mechanisms from the ER calcium stores through specialized ion channels, calcium leak channels, store-operated calcium (SOC) channels on the plasma membrane that respond to changes in ER calcium levels, a calcium pump (sarcoplasmic/endoplasmic reticulum calcium ATP-ase; SERCA) that pumps calcium ions into the ER, and numerous intracellular signaling cascades (Berridge, 2002; Cahalan, 2009; Lefkimmiatis et al., 2009; Mattson et al., 2000; Park et al., 2008; Verkhratsky, 2005). The critical necessity of this process in maintaining high levels of ER calcium is also evident from the severe cellular dysfunction caused by the depletion of ER calcium stores, and the association of such depletion with multiple neurological disorders (Marciniak and Ron, 2006; Mattson et al., 2000; Paschen and Mengesdorf, 2005; Verkhratsky, 2005). Several signaling pathways have been implicated as part of the cellular response to the disruption of ER homeostasis, which are aimed initially at neuroprotection but can eventually trigger cell death if ER dysfunction is severe or prolonged (Xu et al., 2005). Pharmacological agents that block the SERCA pump, for example cyclopiazonic acid (CPA) (Demaurex et al., 1992; Seidler et al., 1989; Uyama et al., 1992) and thapsigargin (Tg) (Lytton et al., 1991; Thastrup et al., 1990), have been used as store depletion agents to investigate some of the consequences associated with disruption of ER calcium homeostasis (Lefkimmiatis et al., 2009; Luik et al., 2008; Marciniak and Ron, 2006; Mattson et al., 2000; Paschen and Mengesdorf, 2005; Verkhratsky, 2005). However, the effects of store depletion on the intrinsic response properties of neurons have been surprisingly unexplored.

The hyperpolarization-activated cation-nonspecific *h* channels are active at rest and modulate numerous neuronal functions including intrinsic excitability, intrinsic oscillatory dynamics, and synaptic integration (Biel et al., 2009). The *h* channel has been shown to be sensitive to multiple neuromodulatory agents and to undergo bidirectional plasticity in response to activity, thus making it a robust cellular target for regulating neuronal response properties at rest (Biel et al., 2009; Brager and Johnston, 2007; Fan et al., 2005; Wang et al., 2003). Consistently, numerous studies have also demonstrated changes in *h* current and consequent changes in intrinsic response properties of hippocampal neurons following pathological conditions (Beck and Yaari, 2008) that induce metabolic stress, like seizures (Chen et al., 2001; Jung et al., 2007; Shin et al., 2008), ischemia (Fan et al., 2008), and behavioral stress (Arnsten, 2009). Additionally, sleep deprivation, a form of nonspecific stress, has also been shown to alter intrinsic excitability of hippocampal neurons through changes in the *h* current (McDermott et al., 2003; Yang et al., 2010).

In this study, we explored the effects of ER calcium store depletion on the intrinsic response properties of hippocampal pyramidal neurons. We show that calcium store depletion in CA1 pyramidal neurons induced a persistent, perisomatic reduction in intrinsic excitability mediated through an increase in the density of functional *h* channels coupled by a depolarizing shift to the *h* channel activation curve. We also found that cytoplasmic calcium elevation through the activation of inositol triphosphate receptors ($InsP_3Rs$) and SOC channels and the activation of the protein kinase A (PKA) pathway were essential for this form of plasticity. Our results suggest roles for the ER calcium stores and SOC channels in the modulation of intrinsic response properties of a neuron. We postulate that this form of depletion-induced intrinsic plasticity represents a neuroprotective mechanism that reduces excitability after depletion of stores triggered through altered network activity during pathological conditions.

RESULTS

CPA, a specific and reversible blocker of the SERCA pump (Seidler et al., 1989; Uyama et al., 1992), was used as a store depletion agent (Demaurex et al., 1992). Unless otherwise stated, store depletion was induced through treatment of slices with 20 μM CPA for 10 min after establishment of stable baselines of the measured parameters (Figures 1A and 1B).

Store Depletion Alters Intrinsic Response Dynamics and Reduces Intrinsic Excitability

We assessed the effects of store depletion on various measurements (Figure 1 and Table 1) associated with the intrinsic response dynamics and excitability of a neuron. Long-current pulses were used to measure steady-state input resistance (R_{in}) and firing properties (Figures 1C and 1D), whereas the *Chirp15* stimulus (Figure 1B) was used to assess frequency-dependent intrinsic response properties (Figures 1F–1H) and a series of α current waveforms (Figure 1I) was injected to assess postsynaptic integrative properties of the neuron (Narayanan and Johnston, 2007, 2008). We found a significant reduction in R_{in} and the number of action potentials fired for a given current injection at 40 min after store depletion (Figures 1, 2, and S1 [available online] and Table 1).

This reduction in intrinsic excitability was also reflected in the impedance measurements, with effects primarily at the lower frequencies (Figures 1G and S1). Accompanying this reduced excitability were increases in the neuron's optimal response frequency (f_R), resonance strength (Q), and total inductive phase (Φ_L), and reductions in the maximal impedance amplitude ($|Z|_{max}$) and temporal summation (Figures 1, 2, and S1 and Table 1). To confirm these results, we repeated the experiment with a structurally distinct and irreversible SERCA pump inhibitor and store depletion agent, Tg (Lytton et al., 1991; Thastrup et al., 1990), and observed identical changes (Figure 2).

When does the *induction* of depletion-induced plasticity occur, and how long does it persist? To answer these questions, we conducted two sets of experiments. First, we extended CPA treatment to span the entire experimental period after the initial 5 min baseline (Figure S2) and found that the amount and direction of plasticity in all measured parameters were not significantly different from that resulting from treating the slice with CPA for only 10 min (Figure S2). From this we concluded that the induction of plasticity occurred at wash-in of CPA and not at washout, and that CPA does not significantly alter the plasticity profile beyond the initial induction period. In a second set of experiments, we treated the slice with CPA only for 10 min, but extended the posttreatment recording period to 70 min, rather than the default 40 min (Figure S3A). We found that the amount and direction of plasticity at 70 min in all measured parameters were not significantly different than those at 40 min, indicating that the plasticity persisted for more than 1 hr after CPA treatment (Figure S3).

Depletion-Induced Changes Were Perisomatic

The locus of plasticity in neuronal ion channels can be either spatially restricted (Frick et al., 2004; Wang et al., 2003) or widespread (Narayanan and Johnston, 2007, 2008), depending on various factors including induction mechanisms, specific ion channels, and signaling pathways. Although our results suggested depletion-induced plasticity in intrinsic response properties as measured at the soma (Figures 1 and 2), the spread of this plasticity into the dendritic tree was unknown. We addressed this question by measuring changes in intrinsic response properties and excitability across the dendritic tree, while following the same protocol for depletion using CPA. Depletion experiments performed through long-term recordings from the apical dendritic trunk, up to around 290 μm away from the soma, established the perisomatic nature of the plasticity. Specifically, the amount of plasticity measured at the dendrites was significantly less than that observed in the soma (Figure 3). It may be noted that firing frequency obtained with long-current pulses was still reduced as measured at dendritic sites, because these are back-propagating action potentials initiated near the soma, where the excitability was reduced following store depletion (Figure 3).

An outstanding question was whether depletion-induced plasticity was just a phenomenon associated with the process of whole-cell patch-clamping the neuron. To address this, we designed an experiment where the 10 min CPA treatment period preceded whole-cell patch-clamping by at least 30 min. The control group of slices received no CPA treatment but was identical to the CPA treatment group in all other aspects (Figure S4A). When we performed somatic recordings from either group and assessed basic cellular properties, we found that the expression of plasticity was still present (Figure S4). Thus, depletion-induced plasticity was expressed even when CPA treatment preceded whole-cell patch-clamp recordings.

An Increase in the *h* Current-Mediated Depletion-Induced Changes in Response Dynamics

Which ion channel mediated depletion-induced plasticity in response dynamics and excitability? We assessed a constellation of measurements associated with intrinsic excitability and response dynamics and depletion-induced changes in each of them, obtained from somatic recordings (see Table 1). The direction of changes in all impedance-related measurements (f_R, Q, Φ_L, $|Z|_{max}$), the observation that the plasticity was predominantly at lower frequencies, the increase in the percentage of sag (Sag) and depolarization of the resting membrane potential (RMP), and

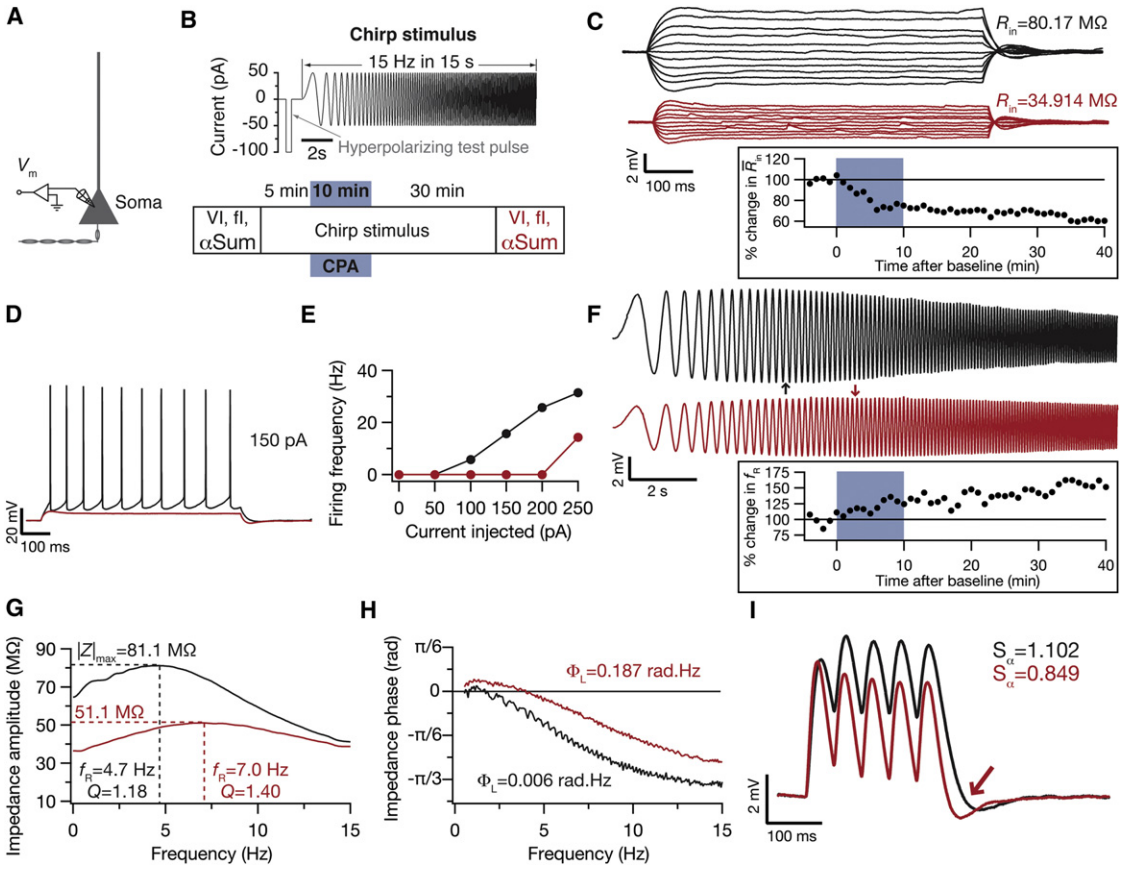

Figure 1. Typical Experiment Demonstrating Plasticity in Intrinsic Excitability and Resonance Properties following the Depletion of Intracellular Calcium Stores

(A) Schematic of the somato-apical trunk depicting the experimental setup for assessing plasticity in intrinsic excitability and resonance properties. Voltage responses (V_m) of the soma to various current stimuli were recorded.

(B) Top: *Chirp15* stimulus used for assessing impedance properties of the cell. The neuron's response to the initial short hyperpolarizing pulse of 100 pA amplitude provided a measure of the neuron's input resistance, while the response to the *Chirp15* stimulus provided the impedance amplitude and phase profiles of the neuron. Bottom: Experimental protocol for assessing the role of store depletion in excitability and resonance properties. The blue patches represent CPA treatment period.

(C) Voltage responses of the cell to constant current pulses of 700 ms duration, varying in amplitude from –50 pA to +50 pA before (black) and after (red) CPA treatment. R_{in}, measured from the steady-state voltage deflections of each of these traces, was reduced after CPA treatment. Inset below: Time course of change in $\overline{R}_{in}$; blue patches represent CPA treatment period.

(D) Example voltage traces recorded by somatically injecting 150 pA depolarizing current before (black) and after (red) CPA treatment indicated a reduction in the number of action potentials fired after CPA treatment.

(E) Graph depicting action potential firing frequency measured by injecting depolarizing current pulses of various amplitudes (0–250 pA) before (black) and after (red) CPA treatment.

(F) Voltage responses of the neuron to the *Chirp15* stimulus during the baseline period (black) and after CPA treatment (red). Arrows in corresponding colors indicate the location of maximal response in each trace. Inset below: Time course of change in f_R; blue patches represent CPA treatment period.

(G) Impedance amplitude as a function of frequency computed from correspondingly color-coded traces in (F). Forty minutes after CPA wash-in, there was an increase in f_R (compare dotted lines) and resonance strength with respect to their baseline values.

(H) Impedance phase as a function of frequency computed from correspondingly color-coded traces in (F). Forty minutes after CPA wash-in, there was an increase in total inductive phase Φ_L (compare area of the two plots above the zero line) with respect to its baseline value.

(I) Voltage responses of the cell to five α-EPSC injections at 20 Hz before (black) and after (red) CPA treatment. A reduction in the amplitude of the last pulse and an increase in the amount of rebound following the last pulse (red arrow) may be noted. All voltage traces and data in this figure were obtained from the same neuron.

the reductions in R_{in}, firing frequency, and temporal summation were all consistent with a depletion-induced increase in the *h* current (Brager and Johnston, 2007; Fan et al., 2005; Magee, 1998; Narayanan and Johnston, 2007, 2008). To test this hypothesis, we performed the standard depletion experiment with 20 μM of the *h* channel blocker ZD7288 added to the recording pipette. In the presence of ZD7288, none of the measurements changed significantly, indicating that plasticity did not express (Figure 4). Thus, physiologically relevant measurements (Figures 1, 2, 3, and S1 and Table 1) and pharmacological evidence

Table 1. Measurements Sensitive to Changes in *h* Channels, and Their Values before and after CPA Treatment, Indicate an Increase in the *h* Current after CPA Treatment

Measurement (Units)	Before CPA	After CPA	Significance
Resting membrane potential (mV)	–61.82 ± 0.49	–56.74 ± 1.06	$p < 0.001$
Input resistance, R_{in} (MΩ)	71.88 ± 5.82	46.37 ± 5.87	$p < 0.005$
Sag (%)	19.43 ± 1.38	24.6 ± 1.12	$p < 0.05$
Firing frequency	–	significantly reduced after CPA	Figure 2
Resonance frequency, f_R (Hz)	4.026 ± 0.27	6.06 ± 0.22	$p < 0.001$
Resonance strength, Q	1.16 ± 0.016	1.36 ± 0.037	$p < 0.005$
Total inductive phase, Φ_L (rad.Hz)	0.0296 ± 0.003	0.167 ± 0.035	$p < 0.005$
Maximal impedance amplitude, $\|Z\|_{max}$ (MΩ)	82.03 ± 8.69	66.13 ± 6.45	$p < 0.01$
Impedance amplitude, $\|Z\|$ versus frequency	–	after CPA, $\|Z\|$ predominantly reduces at lower frequencies	Figure S1
Summation ratio of α−EPSPs, S_α	1.16 ± 0.047	0.87 ± 0.017	$p < 0.01$

Significance was computed with paired Student's t test. All values are mean ± SEM. RMP, resting membrane potential. n = 7 for all parameters, which were measured from the same neurons using somatic recordings, before and 40 min after wash in of 20 μM CPA for 10 min.

(Figure 4) pointed toward an increase in the *h* current as the mediator of the observed changes in intrinsic response dynamics and excitability.

Perisomatic Plasticity Was Larger at More Depolarized Voltages

If the *h* current were the mediator of plasticity, then, given that *h* channel activation increases with hyperpolarization, the measured amount of plasticity in intrinsic properties should be higher at hyperpolarized voltages (Brager and Johnston, 2007; Narayanan and Johnston, 2008). To confirm this, we estimated R_{in} and f_R at multiple voltages before and 40 min after CPA wash-in (Figure 5). Surprisingly, we found that for both the measurements, the amount of plasticity was higher at more depolarized voltages than at hyperpolarized voltages (Figure 5; also see Figure S4). These results led us to ask whether the amount of plasticity in dendrites could be different at voltages other than the RMP, where there was significantly less dendritic plasticity (Figure 3). To answer this question, we recorded from dendrites and measured f_R and R_{in} and multiple voltages before and after CPA treatment (Figure 5). These experiments confirmed our results at RMP, and established that plasticity in dendrites was significantly lower than that at the soma at all measured voltages (Figure 3). Thus, depletion-induced plasticity was perisomatic and had a voltage profile that was biased toward more depolarized voltages.

Our experiments at multiple voltages were designed with the observation that plasticity mediated by *h* channels should be higher at hyperpolarized voltages. Our results, however, state exactly the opposite, showing a higher amount of plasticity at depolarized voltages (Figures 5 and S4). Thus, the question arises as to how the *h* channel dependence of the plasticity (Table 1, Figure 4) and its bias toward depolarized voltages (Figure 3) reconcile with one another. In order to answer this question and to understand the distance-dependent (Figures 2 and 3) and voltage-dependent (Figure 3) profiles of the depletion-induced plasticity, we employed a multicompartmental, morphologically realistic, 3D neuronal model (Figure 5H), which had passive and active properties as in an earlier model (Narayanan and Johnston, 2007). Employing this "base model," we found that a depolarizing shift in half-maximal activation voltage, $V_{1/2}$, accompanied by an increase in maximal *h* conductance density, $\bar{g}_h$, of only somatic *h* channels, were together required to match experimentally observed voltage- and distance-dependent plasticity profiles (compare experimental results in Figures 5C–5E with simulation results in Figures 5I–5K; also see Figure S5). While a shift in $V_{1/2}$ alone was insufficient to account for such large somatic changes in R_{in} and f_R, an increase in $\bar{g}_h$ alone did not match the voltage-dependent profile of plasticity. Changes in both $\bar{g}_h$ and $V_{1/2}$ were required only in somatic *h* channels for matching simulated outcomes with the experimentally observed perisomatic nature of plasticity (Figures 3, 5, and S5). Thus, our simulations suggest that an increase in conductance density of somatic *h* channels accompanied by a depolarizing shift in their activation curve can explain the voltage- and distance-dependent profiles of depletion-induced plasticity.

Depletion-Induced Increase in I_h Is Mediated by an Increase in Density of Functional *h* Channels and a Depolarizing Shift to Its Activation Curve

Physiological measurements (Table 1) and the use of pharmacological agents (Figure 4) suggested that the plasticity in intrinsic properties was related to an increase in the *h* current. Our simulations based on experiments at multiple voltages (Figure 5) suggested that an increase in the number of somatic *h* channels coupled with a change in their gating properties could explain our experimental results. These experiments and simulations, although consistent with one another, form only indirect and inferential proofs for the involvement of the *h* current in depletion-induced plasticity. To assess directly the role of the *h* channels in depletion-induced plasticity and to test our simulation predictions, we performed cell-attached patch-clamp recordings from the soma and dendrites of CA1 pyramidal neurons treated with CPA. We then compared the *h* conductance density and gating properties obtained from these recordings with

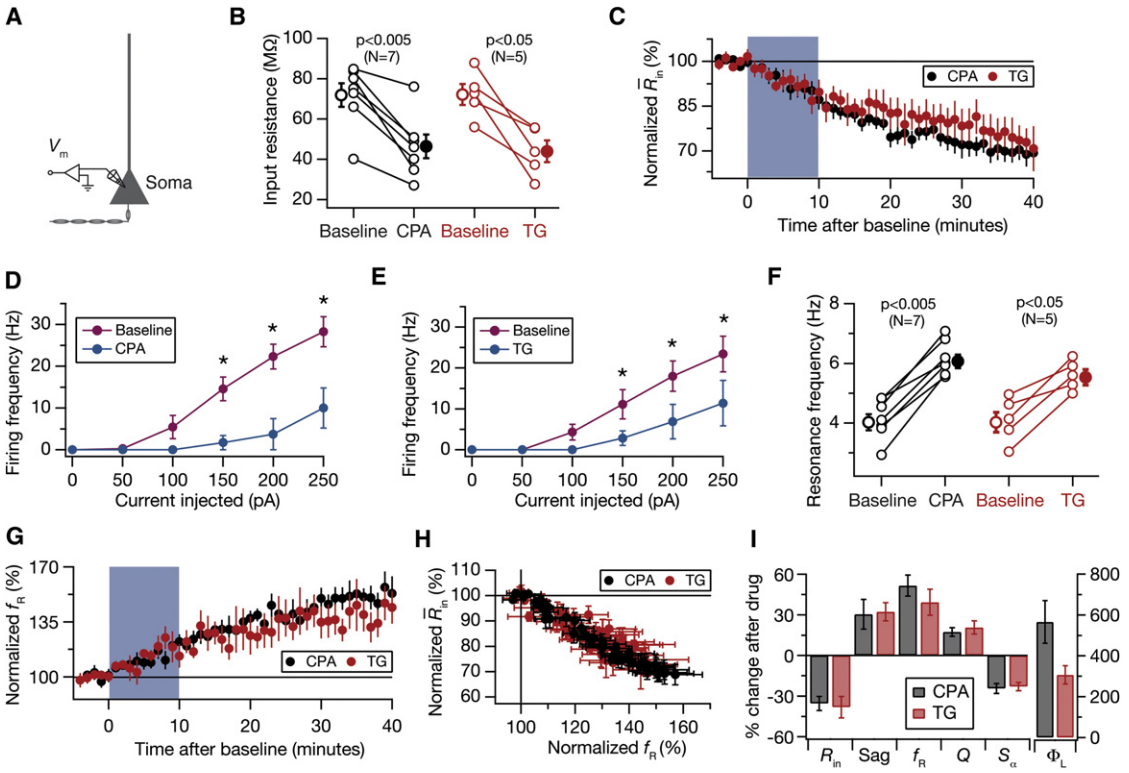

Figure 2. Depletion of Intracellular Calcium Stores through Either Cyclopiazonic Acid or Thapsigargin Induced Significant Plasticity in Intrinsic Excitability and Resonance Properties

(A) Schematic of the somato-apical trunk depicting the experimental setup for assessing depletion-induced plasticity in intrinsic excitability and resonance properties. (B) Population plots of R_{in} measured before (Baseline; open circles) and 40 min after (CPA or Tg; solid circles) cyclopiazonic acid (CPA) or Thapsigargin (Tg) treatment show significant reductions (paired Student's t test; CPA: Baseline: 71.8 ± 5.8 MΩ, CPA: 46.4 ± 5.8 MΩ; Tg: Baseline: 72.2 ± 5.2 MΩ, Tg: 43.9 ± 5.3 MΩ) after CPA or Tg treatment. (C) Time courses of normalized $\overline{R}_{in}$ during CPA or Tg treatment experiments. Blue patches in (C) and (G) represent CPA or Tg treatment period. (D and E) Population plots of action potential firing frequency as a function of injected current to the soma establish significant reductions after CPA (D) or Tg (E) treatment (Baseline: magenta; 40 min after Tg: cyan). *p < 0.05, paired Student's t test. (F) Population plots of f_R measured before (Baseline; open circles) and 40 min after (CPA or Tg; solid circles) CPA or Tg treatment show significant increases in f_R (paired Student's t test; CPA: Baseline: 4.02 ± 0.27 Hz, CPA: 6.06 ± 0.22 Hz; Tg: Baseline: 3.89 ± 0.33 Hz, Tg: 5.52 ± 0.26 Hz) after CPA or Tg treatment. (G) Time courses of normalized f_R during CPA or Tg treatment experiments. (H) Relationship between changes in f_R and $\overline{R}_{in}$ during CPA treatment experiments establish the correlations between these two measurements during the course of the experiment. R = –0.984 (CPA), –0.921 (Tg), Pearson's correlation test. (I) Summary plot of percentage changes in various measurements sensitive to the *h* current, at 40 min after CPA or Tg treatment, relative to respective baseline values. After CPA or Tg treatment, within the respective group, all measurements were significantly different from their respective baseline values (p < 0.05; paired Student's t test), whereas none of the measurements had their percentage changes significantly different across the two groups (p > 0.1; Mann-Whitney test). Error bars = SEM.

those from neurons under standard ACSF (Figure 6). We found that the $V_{1/2}$ of the *h* channel activation curve underwent a depolarizing shift of around 8 mV (Figures 6B–C) and the *h* conductance density increased significantly (Figures 6E and 6F) after CPA treatment. Cell-attached recordings from CA1 pyramidal dendrites showed no significant differences in conductance density or gating properties before and after CPA treatment (Figure 6), confirming that the plasticity is perisomatic (Figure 4). Finally, we also confirmed that the vehicle used for dissolving CPA, DMSO, did not alter *h* conductance density or its gating properties (Figure 6). Thus, based upon plasticity in physiologically relevant measurements (Figures 1, 2, and 3 and Table 1), pharmacological analysis (Figure 4), morphologically precise computer simulations (Figure 5), and direct recordings of the *h* current (Figure 6), we conclude that depletion-induced intrinsic plasticity is perisomatic and is mediated by an increase in density of functional *h* channels coupled with changes to *h* channel gating properties.

Depletion-Induced Elevation in Cytoplasmic Calcium Is Necessary for Plasticity of Intrinsic Properties

Calcium store depletion, by its very definition, is a calcium-dependent phenomenon and is associated with calcium entry into the cytoplasm from the stores and through the plasma membrane (Cahalan, 2009; Parekh and Putney, 2005; Verkhratsky, 2005). We thus assessed whether the plasticity in intrinsic properties was dependent on calcium by performing depletion experiments with 20 mM of the fast calcium chelator BAPTA in the recording pipette. We found that plasticity in all measured parameters was blocked in the presence of intracellular BAPTA (Figures 7B–7D), emphasizing the necessity of cytoplasmic calcium elevation for the manifestation of this form of plasticity.

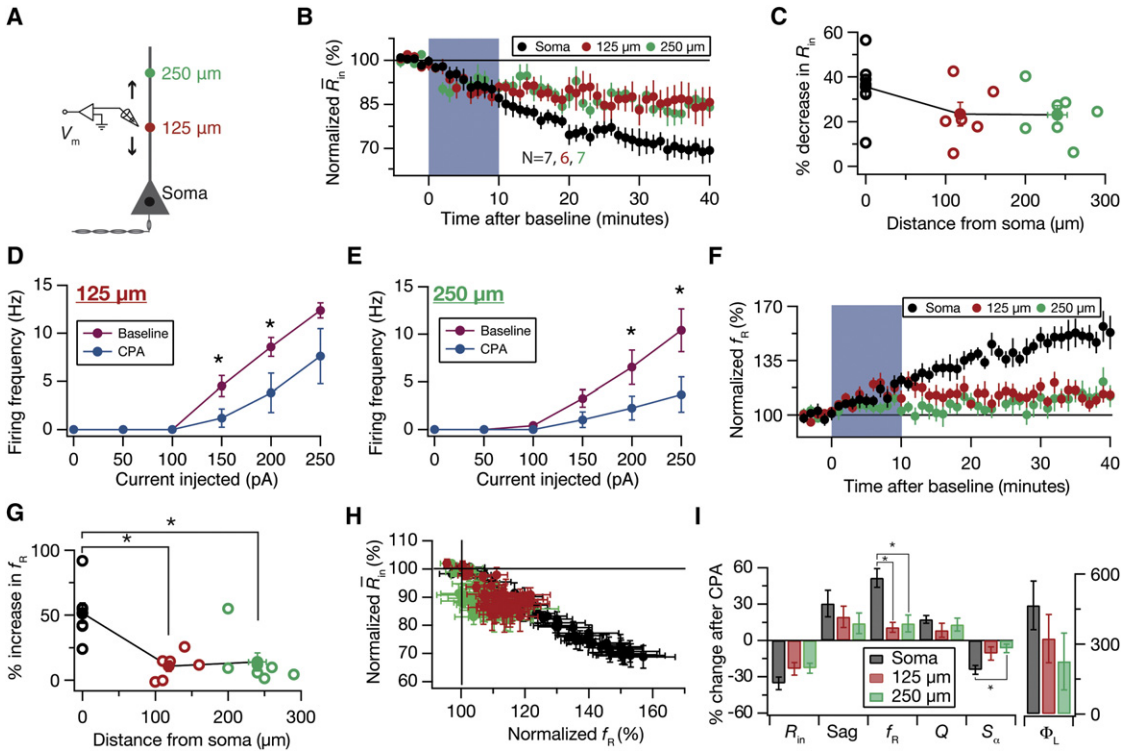

Figure 3. CPA-Induced Plasticity in Intrinsic Excitability and Resonance Properties Was Higher at the Soma Than in the Dendrites

(A) Schematic of the somato-apical trunk depicting the experimental setup for assessing plasticity in intrinsic excitability and resonance properties. Voltage responses (V_m) of the soma and dendrites at various distances (up to approximately 300 μm from the soma) to various current stimuli were locally recorded using a whole-cell patch-clamp electrode. Recordings along the somato-apical trunk are binned into three subpopulations (Soma, 125 μm, and 250 μm) depending on the distance of the recording location from the soma. Colors of markers along the somato-apical trunk serve as codes for corresponding subpopulations in (B)–(I). The protocol for the experiments was the same as that shown in Figure 1B. (B) Time courses of normalized $\overline{R}_{in}$ during CPA treatment experiments (R_{in} values: 125 μm: Baseline: 53 ± 5 MΩ, CPA: 41 ± 5 MΩ; p = 0.03; 250 μm: Baseline: 51 ± 6 MΩ, CPA: 38 ± 4 MΩ; p = 0.0068, paired Student's t test). Blue patches in (B) and (F) represent CPA treatment period. (C) Scatter plot of data in (B). Each open circle represents the magnitude of change, at 40 min after CPA wash-in, relative to the respective baseline value of R_{in} in a given experiment. The solid circles represent the average distance and average plasticity for the three populations. Percentage reduction in R_{in} at 40 min after CPA treatment: Soma: 35% ± 5%, 125 μm: 23% ± 5% at 123 ± 9 μm, 250 μm: 23% ± 4% at 240 ± 1 μm. Percentage reductions across the three subpopulations were not significantly different, with Kruskal Wallis test. (D and E) Population plots of action potential firing frequency as a function of locally injected current to the dendrites indicate significant reductions after CPA treatment in dendrites around 125 μm (D) and 250 μm (E) (Baseline: magenta; 40 min after CPA: cyan). *p < 0.05, paired Student's t test. (F) Time courses of normalized f_R during CPA treatment experiments (f_R values; 125 μm: Baseline: 4.63 ± 0.41 Hz, CPA: 5.04 ± 0.30 Hz; p = 0.047; 250 μm: Baseline: 4.41 ± 0.40 Hz, CPA: 5.06 ± 0.54 Hz; p = 0.08, paired Student's t test). (G) Scatter plot of data in (F). Notations are similar to (C). Percentage increase in f_R at 40 min after CPA: Soma: 51.61% ± 7.84%, 125 μm: 10.79% ± 4.12%, 250 μm: 14.01% ± 6.99%. *p < 0.05: Kruskal Wallis test across the three subpopulations followed by Dunn's post hoc test. (H) Relationship between changes in f_R and $\overline{R}_{in}$ during CPA treatment experiments establish the correlations between these two measurements during the course of the experiment. R = –0.984 (Soma), –0.691 (125 μm), –0.697 (250 μm), Pearson's correlation test. (I) Summary plot of percentage changes in various measurements sensitive to the *h* current, at 40 min after CPA wash-in, relative to respective baseline values. After CPA treatment, within the 125 μm subpopulation, all measurements were significantly different from their respective baseline values (p < 0.05); within the 250 μm subpopulation, R_{in}, Q, and Φ_L were significantly different (p < 0.05), while Sag, f_R, and S_α were not significantly different (p > 0.05); paired Student's t test. *p < 0.05, Kruskal Wallis test across the three subpopulations followed by Dunn's post hoc test. Error bars = SEM.

Depletion-Induced Plasticity Was Intrinsic to the Neuron

Cytoplasmic calcium elevation could be achieved through multiple calcium sources, some of which are dependent on network activity. We asked whether synaptic activity played any role in depletion-induced plasticity or whether it was a strictly intrinsic phenomenon. We addressed this question using two different approaches: (1) using synaptic blockers, and (2) introducing CPA in the recording pipette.

For the first set of experiments with synaptic blockers, we followed the default depletion protocol (Figure 1B). While a combination of AMPAR blockers with $GABA_AR$ and $GABA_BR$ blockers in the bath did not alter the expression of depletion-induced plasticity (Figure 7), the presence of NMDAR blockers significantly reduced it (Figure 7). Given this dependence on NMDARs, we next asked whether there was a role for spontaneous synaptic activity by performing depletion experiments in the presence of 1 μM TTX in the bath. We found, however, that there was no significant change in the expression of depletion-induced plasticity in the presence of TTX in the bath (Figure 7). Thus, while spontaneous, action potential-evoked activity was not essential for the manifestation of depletion-induced plasticity, it was possible that CPA in the bath initiated synaptic

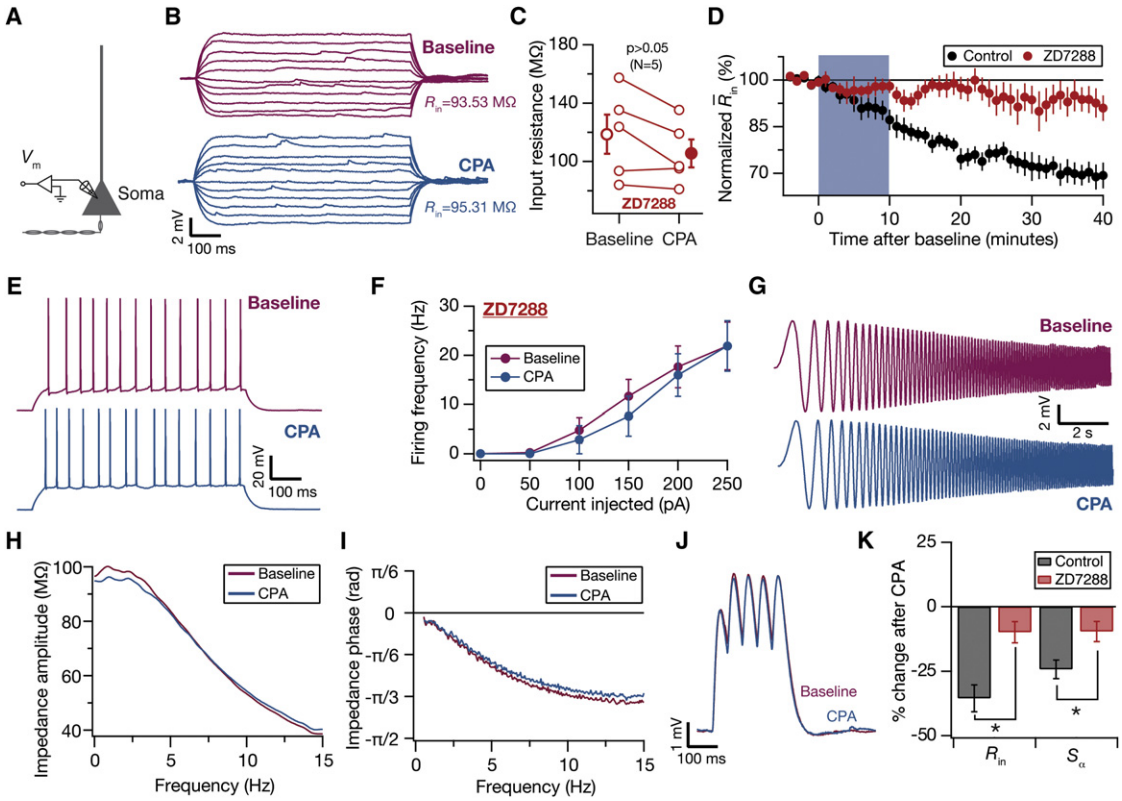

Figure 4. Depletion-Induced Plasticity in Intrinsic Excitability Was Abolished in the Presence of ZD7288

(A) Diagram depicting the experimental setup for assessing the role of *h* channels in depletion-induced plasticity. Voltage recordings at the soma (V_m) were performed with 20 μM ZD7288 in the pipette.

(B) Voltage responses of the cell to constant current pulses of 700 ms duration, varying in amplitude from –50 pA to +50 pA before (magenta) and after (cyan) CPA treatment.

(C) Population plots of R_{in} measured before (Baseline; open circles) and 40 min after (CPA; solid circles) CPA wash-in showing no significant changes (paired Student's t test; Baseline: 119 ± 13 MΩ, CPA: 105 ± 9 MΩ) at 40 min after CPA wash-in.

(D) Time courses of normalized $\overline{R}_{in}$ during CPA treatment experiments. Blue patch represents CPA treatment period.

(E) Example voltage traces recorded by somatically injecting 200 pA depolarizing current before (magenta) and after (cyan) CPA treatment.

(F) Population plots of action potential firing frequency as a function of injected current to the soma establish the absence of any significant change (paired Student's t test) at 40 min after CPA wash-in (Baseline: magenta; 40 min after CPA: cyan).

(G) Voltage responses of the neuron to the *Chirp15* stimulus during the baseline period (magenta) and after CPA treatment (cyan).

(H and I) Impedance amplitude (H) and phase (I) as functions of frequency computed from correspondingly color-coded traces in (G). Across the populations, f_R and *Q* remained close to unity through the course of the experiment, and were not significantly different before and 40 min after CPA wash-in (f_R: Baseline: 0.76 ± 0.06 Hz, CPA: 0.81 ± 0.12 Hz, $p > 0.5$; *Q*: Baseline: 1.04 ± 0.01, CPA: 1.035 ± 0.01, $p > 0.5$; paired Student's t test). Φ_L remained close to zero throughout the course of the experiment, and was not significantly different before and 40 min after CPA wash-in (Φ_L: Baseline: 0.0134 ± 0.0069 rad.Hz, CPA: 0.0168 ± 0.0093 rad.Hz, $p > 0.3$; paired Student's t test).

(J) Voltage responses of the cell to five α-EPSC injections at 20 Hz before (black) and after (red) CPA treatment, showing no significant changes between them. All voltage traces in this figure were obtained from the same neuron.

(K) Summary plot of percentage changes in various measurements sensitive to the *h* current, 40 min after CPA wash-in without (Control) and with (ZD7288) ZD7288 in the pipette, relative to respective baseline values. *$p < 0.05$; Mann-Whitney test.

Error bars = SEM.

release through store depletion in axon terminals (Verkhratsky, 2005), which in turn activated NMDARs.

In our second set of experiments, to rule out the role of such presynaptic release, we asked whether inclusion of CPA in the pipette was sufficient to elicit depletion-induced plasticity. To do this, we included 20 μM CPA in the recording pipette, and monitored various measurements over a recording period of 45 min, without adding CPA to the standard extracellular solution. The direction and amount of changes in measurements with CPA in the pipette were not significantly different from those obtained with CPA in the bath (Figures 7 and S6). Remarkably, this plasticity induced by the inclusion of CPA in the pipette was not affected by the presence of NMDAR blockers in the bath (Figures 7 and S6). Together, these experiments establish that depletion-induced plasticity can be strictly intrinsic to the neuron, but that synaptic activity and NMDARs could play a role in the manifestation of the plasticity in a functioning neural network.

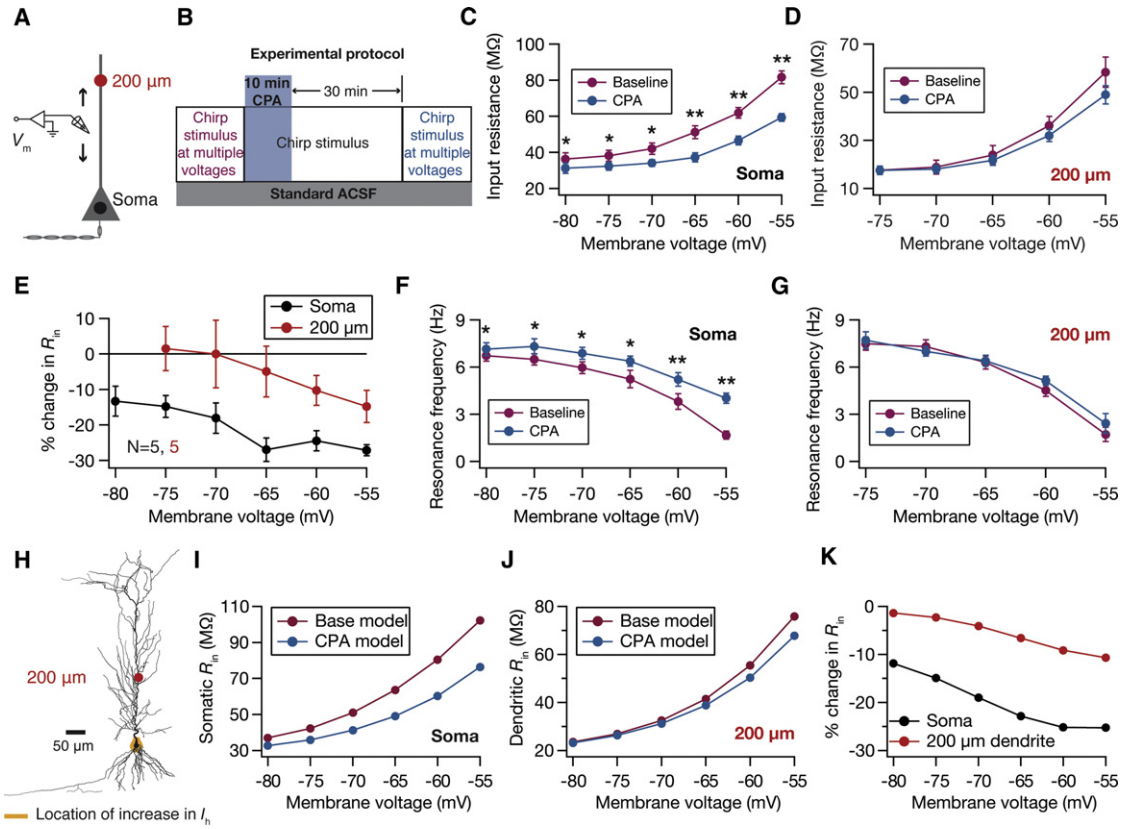

Figure 5. Perisomatic Depletion-Induced Plasticity in Intrinsic Excitability and Resonance Properties Was Higher at More Depolarized Voltages

(A) Schematic of the somato-apical trunk depicting the experimental setup for assessing voltage-dependence of depletion-induced plasticity. Voltage responses (V_m) of the soma and dendrites at various distances (up to around 260 µm from the soma) to various current stimuli were locally recorded using a whole-cell patch-clamp electrode. Recordings along the somato-apical trunk are binned into two subpopulations (Soma, and 200 µm dendrite) depending on the distance of the recording location from the soma. Colors of markers along the somato-apical trunk serve as codes for corresponding subpopulations in (C)–(G). (B) Diagram depicting the experimental protocol for assessing depletion-induced plasticity at multiple voltages. Whole-cell recordings were performed to measure the responses of the soma/dendrite to the *Chirp15* stimulus at multiple "holding" voltages. Then, the neuron was brought to RMP and the slice was treated with 20 µM CPA for 10 min (blue patch), and responses to the *Chirp15* stimulus were continuously recorded until 40 min after CPA wash-in. Finally, the responses of the soma/dendrite to the *Chirp15* stimulus at multiple holding voltages were measured. Estimates of $\overline{R}_{in}$ and f_R were obtained from the responses to Chirp15 stimulus, and plasticity was assessed by comparing the measurements before and after CPA. (C) When measured at multiple voltages, $\overline{R}_{in}$ was significantly reduced at all voltages after CPA treatment. *$p < 0.05$; **$p < 0.005$, paired Student's t test. (D) When measured at multiple voltages, $\overline{R}_{in}$ of dendrites around 200 µm (206 ± 15.03 µm) away from the soma was not significantly different (paired Student's t test) before and after CPA treatment. (E) Plot depicts percentage changes in $\overline{R}_{in}$ obtained for the "Soma" and "200 µm dendrite" groups computed from corresponding paired values plotted in (C) and (D), respectively. (F and G) When measured at multiple voltages, f_R was significantly higher at all measured voltages after CPA treatment at the soma (F), but not significantly different at any of measured voltages for dendrites around 200 µm from the soma (G). *$p < 0.05$; **$p < 0.005$, paired Student's t test. (H) Projection of the 3D neuronal reconstruction used for multicompartment simulations, depicting a graphical illustration of location of changes in *h* channel properties (orange shade). The apical trunk location at 200 µm, to compare it with experimental measurements in (D), from where the dendritic changes were measured (for J and K) is marked in red. For obtaining the "CPA model," only somatic *h* channels of the "Base model" were altered by (1) a depolarizing shift of 20 mV to the $V_{1/2}$ of *h* channels, and (2) a 10-fold increase in maximal *h* conductance, $\overline{g}_h$. (I–K) Somatic (I) and dendritic (K; at 200 µm distance from the soma) local $\overline{R}_{in}$ as functions of membrane voltage in both the base (magenta) and the CPA (cyan) models. (K) Percentage changes of local $\overline{R}_{in}$ at the soma (black) and the dendrite (red) as functions of membrane voltage in the CPA model in comparison to the base model. The plots were obtained by finding percentage changes of corresponding somatic (I) and dendritic (K) $\overline{R}_{in}$ plots. Error bars = SEM.

Multiple Calcium Sources Contributed to Depletion-Induced Plasticity

If the plasticity were intrinsic to the neuron, what calcium sources would be involved? We employed multiple pharmacological agents to answer this question systematically. First, we performed a set of depletion experiments in the presence of a combination of 10 µM nimodipine and 50 µM $NiCl_2$ to block *L*- and *T*-type calcium channels, respectively. Blockade of these voltage-gated calcium channels (VGCC) did not significantly alter the changes in any of the measured parameters, thus ruling out a role for VGCCs in this plasticity (Figure 7). Next, given that calcium release from stores could be through $InsP_3Rs$, we asked whether these receptors played a role in depletion-induced plasticity. When we performed depletion experiments in the presence of 1 mg/ml heparin, an $InsP_3R$ antagonist, in the pipette, depletion-induced plasticity was blocked, establishing

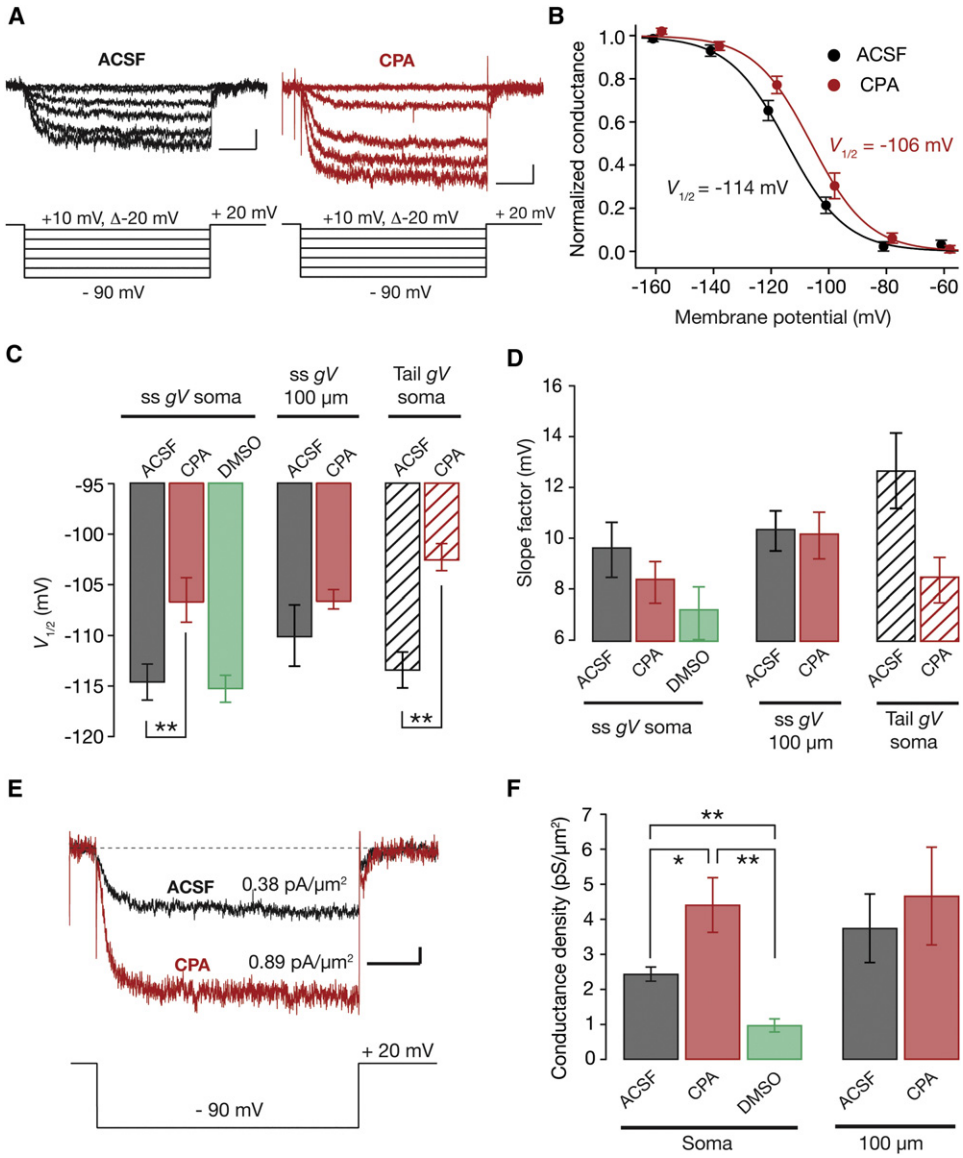

Figure 6. CPA Alters the Biophysical Properties and Density of Somatic *h* Current

(A) Somatic *h* current was measured from ACSF-treated (black traces) or CPA-treated neurons (red traces) with hyperpolarizing step voltage commands ranging from +10 mV to –90 mV in –20 mV increments from a holding potential of +20 mV. All indicated voltages are relative to RMP. Scale bars represent 2 pA and 100 ms.

(B) CPA treatment is associated with an ~8 mV depolarizing shift in the somatic steady-state *gV* (ss *gV*) relationship. Data were described by Boltzmann functions with the following fit parameters: ACSF (black circles) $V_{1/2}$ = –114 mV, *k* = 10.2 mV, CPA (red circles) $V_{1/2}$ = –106 mV, *k* = 9.95 mV.

(C and D) Bar graphs demonstrating the somatic shift in $V_{1/2}$ associated with CPA treatment (C) and the corresponding slope factors (D). CPA treatment (red bars) induced a significant shift in the ss *gV* relationship relative to that of ACSF (black bars) control patches (CPA: –106.5 ± 2.18 mV; ACSF: –114.6 ± 1.78 mV; Student's t test, p = 0.01), whereas treatment with the 0.1% DMSO vehicle (green bars) did not (Student's t test, p = 0.78). Solid bars represent values derived from ss *gV* relationships (ACSF n = 10, CPA n = 10, and 0.1% DMSO n = 3), whereas dashed bars represent a subset of experiments in which *h* current was large enough to determine the *gV* relationship from peak tail currents (ACSF n = 4 and CPA n = 4). CPA treatment did not alter either the $V_{1/2}$ or the slope factor of dendritic *h* channels.

(E) Example currents elicited by maximally activating step hyperpolarizations from ACSF (black trace) and CPA-treated (red trace) neurons demonstrating an increased maximal current density associated with CPA treatment. Currents have been scaled according to the free surface area of the sealed membrane within the pipette (ACSF = 15.4 μm^2 and CPA = 10.6 μm^2) and are representative of the average observed current density. Scale bars represent 0.1 pA/μm^2 and 100 ms, respectively.

(F) CPA treatment (red bar) is associated with a significant increase in the maximal somatic *h* conductance density relative to ACSF (black bar) control (CPA: 4.41 ± 0.78 pS/μm^2, n = 10; ACSF: 2.44 ± 0.20 pS/μm^2, n = 10; Wilcoxon ranked sum test, p = 0.04), whereas the dendritic *h* conductance density is not significantly affected (CPA: 4.67 ± 1.40 pS/μm^2, n = 4; ACSF: 3.75 ± 0.98 pS/μm^2, n = 4; Wilcoxon ranked sum test, p = 0.5). *0.01 < p < 0.05; **p ≤ 0.01.

Error bars = SEM.

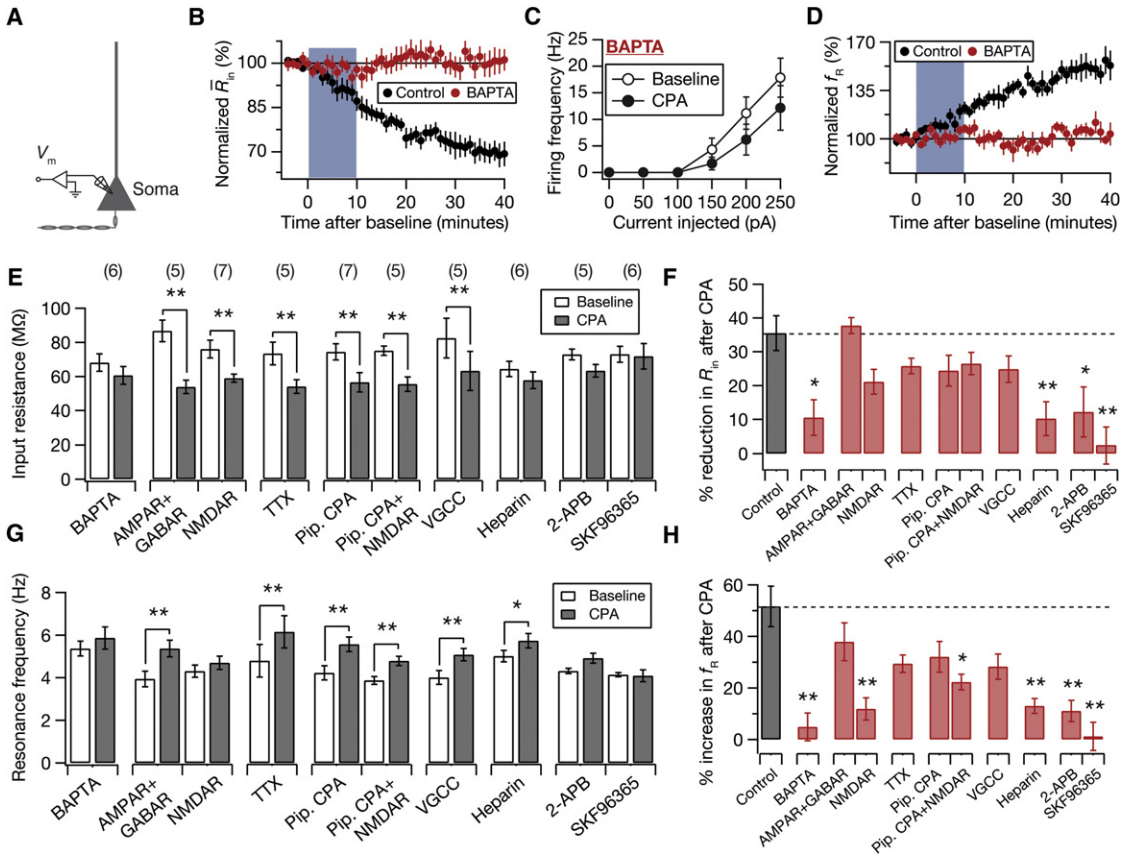

Figure 7. Depletion-Induced Plasticity Was Dependent on the Elevation of Cytoplasmic Calcium Predominantly through $InsP_3Rs$ and SOC Channels

(A) Diagram depicting the experimental setup. Voltage recordings at the soma (V_m) were performed with multiple pharmacological agents in the bath or in the pipette to assess calcium dependence and sources related to depletion-induced plasticity. (B) Time courses of normalized $\bar{R}_{in}$ in experiments performed with 20 mM BAPTA in the recording pipette (red). Blue patch represents CPA treatment period. (C) With 20 mM BAPTA in the recording pipette, population plots of action potential firing frequency as a function of injected current to the soma establish the absence of any significant change (paired Student's t test) at 40 min after CPA wash-in (Baseline: open circles; 40 min after CPA: closed circles). (D) In experiments performed with BAPTA in the pipette (red), time courses of normalized f_R. Blue patch represents CPA treatment period. Values of R_{in} (E) and f_R (G) before (white) and 40 min following (gray) CPA wash-in with various pharmacological agents in the recording pipette or in the bath are shown. *$p < 0.05$; **$p < 0.005$, Student's t test. Corresponding percentage changes in R_{in} (F) and f_R (H), and their comparison to the control case, are also provided. *$p < 0.05$; **$p < 0.005$, Mann-Whitney test. AMPAR+GABAR: AMPAR, $GABA_AR$, and $GABA_BR$ blockers in the recording solution. NMDAR: 50 μM D,L–APV and 10 μM (+)MK801 in the recording solution. TTX: 1 μM tetrodotoxin in the recording solution. Pip. CPA: Experiments performed with 20 μM CPA in the pipette, and not in the recording solution. Pip. CPA+NMDAR: Same as Pip. CPA, but with 50 μM D,L–APV and 10 μM MK801 in the recording solution. VGCC: 10 μM nimodipine and 50 μM $NiCl_2$ in the recording solution. Heparin: 1 mg/ml heparin in the recording pipette. 2-APB: 50 μM 2-APB in the recording solution. SKF96365: 30 μM SKF96365 in the recording solution. Numbers within parentheses in (E) are the number of experiments performed within each of the groups. Error bars = SEM.

a crucial role for $InsP_3Rs$ (Figures 7 and S7). Finally, given that depletion of stores activates SOC entry through the plasma membrane (Cahalan, 2009; Klejman et al., 2009; Luik et al., 2008), we asked whether there was a role for these SOC channels in the manifestation of depletion-induced plasticity. We performed different sets of experiments in the presence of two different pharmacological agents that inhibit SOC channels, 50 μM 2-APB or 30 μM SKF96365. The presence of either inhibitor blocked depletion-induced plasticity (Figures 7 and S7), suggesting SOC channels as a calcium source for the plasticity. Given that 2-APB has also been implicated in the inhibition of $InsP_3Rs$ (Bootman et al., 2002), it provides evidence for the involvement of both $InsP_3Rs$ and SOC channels, while experiments with heparin and SKF96365 provide corroborative confirmation for the involvement of each of these, respectively. Effectively, these results provide evidence for the requirement of a synergistic activation of $InsP_3Rs$ and SOC channels for the manifestation of depletion-induced plasticity (Parekh and Putney, 2005; Woodard et al., 2010).

Depletion-Induced Plasticity Was Dependent on the PKA Pathway

We next asked which downstream signaling pathway led to changes in the *h* current. Previous studies have shown that upregulation of *h* current, through theta burst pairing or firing, occurs through the activation of the CaMKII pathway (Fan

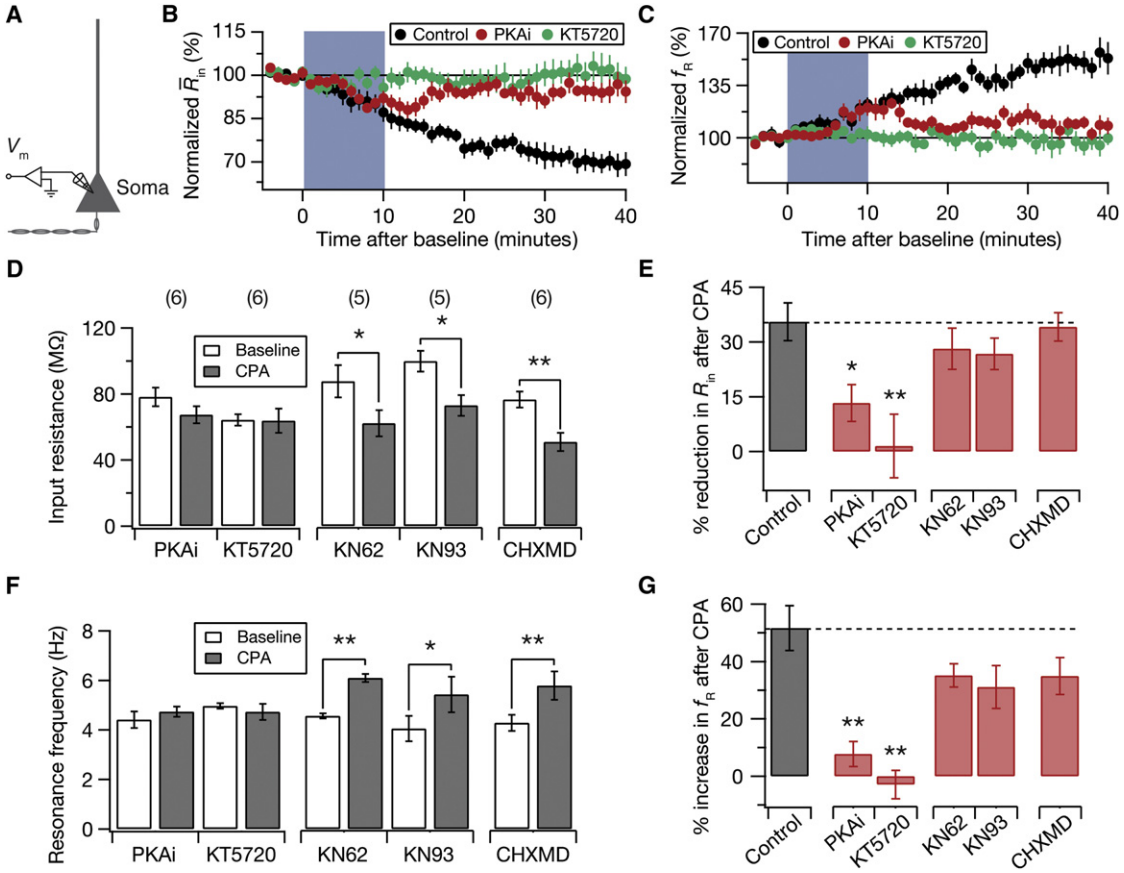

Figure 8. Depletion-Induced Plasticity Was Dependent on the Activation of the PKA Pathway, and Not on the CaMKII Pathway or on Protein Synthesis

(A) Diagram depicting the experimental setup. Voltage recordings at the soma (V_m) were performed with multiple pharmacological agents in the bath or in the pipette to assess downstream mechanisms related to depletion-induced plasticity. Except for experiments in PKAi group, where PKAi was applied through the recording pipette, each of these depletion experiments was performed after preincubation for 30–60 min with the specific pharmacological agent, which is also present in the bath during the course of the experiment. (B and C) In experiments performed with 20 μM PKA inhibitor peptide fragment, PKAi in the pipette (red), or 500 nM KT5720 (green) in the recording solution, time courses of normalized $\overline{R}_{in}$ (B) and f_R (C) showed no significant changes at 40 min following CPA wash-in. Blue patch represents CPA treatment period. Values of R_{in} (D) and f_R (F) before (white) and 40 min following (gray) CPA wash-in with various pharmacological agents in the recording pipette or in the bath are shown. *$p < 0.05$; **$p < 0.005$, Student's t test. Corresponding percentage changes in R_{in} (E) and f_R (G), and their comparison to the control case, are also provided. *$p < 0.05$; **$p < 0.005$, Mann-Whitney test. KN62: 3 μM KN62 in the recording solution. KN93: 10 μM KN93 in the recording solution. CHXMD: 60 μM cycloheximide in the recording solution. Numbers within parentheses in (D) are the number of experiments performed within each of the groups. Error bars = SEM.

et al., 2005). In order to test whether depletion-induced plasticity was dependent on the CaMKII pathway, we used two distinct CaMKII inhibitors, 3 μM KN62 or 10 μM KN93. Our results indicated that depletion-induced plasticity was not dependent on the CaMKII pathway (Figure 8). Recently, it was demonstrated that store depletion activates PKA (Lefkimmiatis et al., 2009). As PKA-dependent modulation of the *h* current is well established (Chang et al., 1991; Frère et al., 2004; Vargas and Lucero, 2002), we asked whether depletion-induced plasticity in *h* current was dependent on the PKA pathway. The use of 20 μM of PKA inhibitor peptide fragment 6–22 in the recording pipette or application of 500 nM of PKA inhibitor KT5720 to the bath abolished depletion-induced plasticity in intrinsic properties (Figures 8 and S8). Finally, we asked whether depletion-induced plasticity was dependent on protein synthesis, using cycloheximide as the protein synthesis inhibitor, and our results suggested that this form of plasticity was independent of protein synthesis (Figure 8). Together, these results establish that depletion-induced plasticity was dependent on the PKA pathway, but not on the CaMKII pathway or on protein synthesis.

DISCUSSION

In this study, we have shown that the depletion of ER calcium stores in rat hippocampal neurons induced a persistent, perisomatic reduction in intrinsic excitability and an accompanying increase in the f_R of the cell. Physiological measurements and the use of pharmacological agents strongly support the conclusion that this plasticity was mediated through changes in *h* channels. We directly confirmed the involvement of *h* channels using

cell-attached recordings and established an increase in density of functional *h* channels and a depolarizing shift to the *h* channel activation curve following treatment with CPA. We also demonstrated that this form of intrinsic plasticity was dependent on elevation of cytoplasmic calcium, with $InsP_3Rs$ and SOC channels contributing to this elevation. Finally, we showed that the plasticity was dependent on the PKA pathway, but not on the CaMKII pathway or protein synthesis.

Physiological Implications

The presence of SOC channels in hippocampal neurons and their activation in response to intracellular calcium store depletion is well established (Klejman et al., 2009). The roles of the ER and the SOC channels in various forms of short- and long-term synaptic plasticity have also been extensively studied (Baba et al., 2003; Mattson et al., 2000; Nishiyama et al., 2000; Verkhratsky, 2005). Our results expand on these roles of the ER and SOC channels to the plasticity of intrinsic neuronal properties by demonstrating that these two sources of calcium may also be involved in altering the properties of voltage-gated ion channels. Through this addition of voltage-gated ion channel plasticity to the already broad-ranging roles of the ER in protein synthesis and maturation and synaptic plasticity, our results further strengthen the postulated role for the neuronal ER network as a conveyor and integrator of dendritic signals (Berridge, 2002; Park et al., 2008). Future studies should thus consider this role of ER calcium in modulating intrinsic properties of neurons, apart from the exploration of the responses of neurons in other brain regions to depletion of stores.

Why would depletion-induced changes in intrinsic properties be perisomatic (Figure 3)? Possible answers come from the higher density of $InsP_3Rs$ located on the ER in the perisomatic region of CA1 pyramidal neurons (Nicolay et al., 2007), on the perisomatic location of SOC channels (Klejman et al., 2009), or on rough ER (Berridge, 2002; Park et al., 2008; Verkhratsky, 2005). What would such perisomatic changes mean physiologically? Because action potential generation occurs perisomatically, the observed plasticity would have a profound effect on the excitability of the neurons, irrespective of the origin of the synaptic inputs (Zhang and Linden, 2003). Further, these perisomatic changes would also alter the transfer properties and somato-dendritic coupling of signals, thus changing the integrative properties of the entire neuron. Thus, both the integrative and the output modules of the single-neuron information processing machinery would be affected by the perisomatic changes induced by store depletion. Such ER-driven reduction in overall intrinsic excitability of a neuron could act as a common neuroprotective mechanism that compensates for network-driven insults incurred by the neuron in pathological conditions (see below).

Mechanisms

Our results suggest that the depletion-induced synergistic activation of $InsP_3Rs$ and the SOC channels (Parekh and Putney, 2005; Woodard et al., 2010) formed the predominant source of calcium for this form of plasticity—inhibiting either of these two sources of calcium blocked plasticity (Figure 7). Further, whereas the plasticity induced by CPA in the bath was suppressed by NMDAR blockers, there was no significant impact of NMDAR blockers when CPA was in the pipette (Figure 7). One possibility is that CPA in the bath also induced calcium release from the stores in the presynaptic terminals, leading to glutamate release and activation of postsynaptic NMDARs, which in turn activated SOC channels and led to a greater elevation of intracellular calcium (Baba et al., 2003). Such a possibility would imply that the amount of plasticity induced by CPA in the pipette (increase in f_R: 32% ± 6%; reduction in R_{in}: 24% ± 4%) would be less than that induced by CPA in the bath (increase in f_R: 51% ± 8%; reduction in R_{in}: 35% ± 5%), which was consistent with our results (Figures 2 and 7). Our results (Figure 8) further demonstrated that this depletion-induced surge in calcium activated PKA downstream (Lefkimmiatis et al., 2009), which in turn led to the modulation of *h* channel properties (Chang et al., 1991; Frère et al., 2004; Vargas and Lucero, 2002). Specifically, our results suggest an increase in the density of functional *h* channels (Figure 6) as the mechanism underlying the observed changes in intrinsic properties (Figure 2) associated with depletion. Future work could elucidate the molecular mechanisms underlying such an increase, as this presents the interesting possibility of surface insertion of *h* channels accompanying CPA treatment. Various isoforms of TRIP8b, an auxiliary subunit of native *h* channels, have been implicated in modulating gating and surface expression of HCN channels (Lewis et al., 2009; Santoro et al., 2009), and could be tested for a possible role in the plasticity described here.

Our results also have implications for the methodology in which store depletion agents have been used in elucidating the mechanistic details of multiple phenomena. It has been traditionally considered that performing a given experiment after depleting the stores would rule out the role of stores in a given phenomenon, as store calcium would not be released from a depleted store. Given that depletion can alter cellular response properties drastically, however, such interpretations and thus the use of depletion agents for studying exclusively store-related phenomenon should be done with extreme caution. It is possible that depletion-induced plasticity in cellular properties could be altering the studied phenomenon, which may have nothing to do with the role of stores per se.

ER Calcium Homeostasis, ER Stress, and Neurological Disorders

Because the ER is responsible for transcription, posttranslational protein modification, and selective transport of proteins to different destinations, it has developed a highly sophisticated system for controlling the quality of the final protein products. Any imbalance of protein handling triggers a specific reaction generally defined as the ER stress response. Because the activity of many intra-ER enzymatic cascades that control protein handling and other ER functions depends on the intraluminal Ca^{2+} concentration, a strong link between ER Ca^{2+} homeostasis, ER stress, and neurodegeneration has been postulated (Mattson et al., 2000; Paschen and Mengesdorf, 2005; Verkhratsky, 2005; Xu et al., 2005). Depletion of ER stores using pharmacological agents like CPA and Tg has been used as an effective tool in elucidating this link and in studying the relationship of ER Ca^{2+} homeostasis to protein synthesis, neurotoxicity, neuronal death, and the

regulation of ER stress markers (Mattson et al., 2000; Paschen and Mengesdorf, 2005; Verkhratsky, 2005). Multiple neurological disorders including epilepsy, ischemia, Huntington disease, and Alzheimer disease have been linked to ER stress and/or altered SOC channel function (Bojarski et al., 2008; Mattson et al., 2000; Paschen and Mengesdorf, 2005; Verkhratsky, 2005).

Additionally, numerous studies have linked changes in *h* current and consequent changes in intrinsic response properties of hippocampal neurons to various pathological conditions (Beck and Yaari, 2008). Specifically, an increase in the *h* current and a consequent reduction in intrinsic excitability have been shown 1–2 days following status epilepticus (Shin et al., 2008), and this increase has been demonstrated to be perisomatic and to be mediated by an increase in *h* channel surface expression. Following this initial period where there is a reduction of excitability, there is a later increase in excitability owing to a reduction in *h* channel surface expression primarily in dendrites. Furthermore, the long-term deleterious effects of status epilepticus, including neuronal loss, are well established (Sankar et al., 1998). The biphasic time course of these changes in *h* channels has similarities to the biphasic nature of the response of the cell to the disruption of ER homeostasis. Specifically, cellular response to the disruption of ER homeostasis is aimed initially at neuroprotection, but can eventually trigger cell death if ER dysfunction is severe or prolonged (Mattson et al., 2000; Paschen and Mengesdorf, 2005; Verkhratsky, 2005; Xu et al., 2005). Based on these observations, we postulate that the depletion-induced intrinsic plasticity reported here is a neuroprotective mechanism that reduces excitability after depletion of stores triggered through altered network activity during pathological conditions. A testable hypothesis that follows this postulate is that the signaling mechanisms underlying the cellular response to ER dysfunction mediate the neuronal response to disorders like epilepsy, and the consequent modulation of ion channels over a time period.

In conclusion, we have demonstrated that intracellular calcium store depletion in rat hippocampal neurons induces a persistent, perisomatic increase in the density of functional *h* channels, mediated by calcium elevation through the activation of $InsP_3Rs$ and SOC channels and the PKA pathway. These results effectively link store depletion to neuronal excitability through SOC channels and $InsP_3Rs$, and could provide useful insights into the role of intracellular stores in neuronal function, plasticity, and dysfunction (Lefkimmiatis et al., 2009; Marciniak and Ron, 2006; Parekh and Putney, 2005; Verkhratsky, 2005). An important new direction would be to explore the relationship between the signaling mechanisms associated with such depletion-induced plasticity and those associated with the neurological disorders of epilepsy and Alzheimer disease. Such experiments would test our postulate that this form of depletion-induced intrinsic plasticity is a neuroprotective mechanism that reduces excitability after depletion of stores triggered through altered network activity during pathological conditions.

EXPERIMENTAL PROCEDURES

Detailed experimental procedures are provided in the Supplemental Information.

Electrophysiology

Near-horizontal 350 μm hippocampal slices were prepared from 4- to 9-week-old male Sprague Dawley rats using standard procedures (Narayanan and Johnston, 2008). Whole-cell patch recordings in current-clamp mode were made from the soma or the dendrites of CA1 pyramidal neurons using a Dagan IX2-700 amplifier. Signals were filtered at 5 kHz and sampled at 10–50 kHz. Recordings were made at 33°C–35°C. Electrode resistance was 4–6 MΩ for somatic recordings and 5–7 MΩ for dendritic recordings. An estimate of the neuron's input resistance (denoted by $\overline{R}_{in}$) was measured from the steady-state response of the cell to a 100 pA hyperpolarizing current pulse, which was also used to monitor and compensate for changes in series resistance. Experiments were discarded if the access resistance crossed 25 MΩ for somatic recordings, or 40 MΩ for dendritic recordings. Data acquisition and analysis were performed with custom-written software in the IGOR Pro environment (Wavemetrics Inc., USA).

Measurements

R_{in} was measured as the slope of a linear fit to the steady-state *V–I* plot obtained by injecting subthreshold current pulses of amplitudes spanning –50 pA to 50 pA. The stimulus used for characterizing impedance parameters was a sinusoidal current of constant amplitude, a *Chirp* stimulus, with its frequency linearly spanning 0–15 Hz in 15 s (*Chirp15*; Figure 4A). The magnitude and phase of the ratio between the Fourier transform of the voltage response and the Fourier transform of the *Chirp* stimulus formed the impedance amplitude and phase profiles, respectively. The frequency at which the impedance amplitude reached its maximum was the f_R. *Q* was measured as the ratio of $|Z|_{max}$ to the impedance amplitude at 0.5 Hz. Total inductive phase (Φ_L) was measured as the area under the positive segment of the impedance phase profile (Narayanan and Johnston, 2007, 2008). The amplitude of the *Chirp15* stimulus was held constant (100 pA, peak-to-peak) throughout the course of the experiment. Sag was measured from the voltage response of the cell to a hyperpolarizing current pulse of 100 pA, and was defined as $100^*(1 - V_{ss}/V_{peak})$, where Vss was the steady-state voltage deflection from baseline and V_{peak} was the peak voltage deflection from baseline. α-EPSPs were evoked by a current injections of the form $I_\alpha = I_{max}$ t exp (–αt), with α = 0.1/ms. Temporal summation ratio (S_α) in a train of five α-EPSPs at 20 Hz was computed as E_{last}/E_{first}, where E_{last} and E_{first} were the amplitudes of last and first α-EPSPs in the train, respectively. In measuring temporal summation, the amplitude of a single EPSP was set the same (around 4–5 mV) before and after CPA treatment. This was done by changing I_{max}, and was necessary because of changes in R_{in} after CPA treatment (Figures 1 and 2). Voltages have not been corrected for the liquid junction potential (~8 mV).

Cell-Attached Recordings

Somatic and dendritic I_h were measured in the cell-attached patch-clamp configuration using an Axopatch 200B amplifier (Molecular Devices Inc., CA). In experiments involving the application of CPA (or DMSO), seals were formed 30–60 min following the introduction of CPA (or DMSO) through the bath. Current recordings were filtered at 2 kHz and sampled at 10 kHz. Passive leak and capacitive transients were subtracted off-line using a scaled leak trace elicited by 10 mV depolarizations from the holding potential. Typically, between 100 and 220 individual leak traces were averaged in order to minimize the addition of noise to the leak subtracted current waveforms. Only experiments with a maximal conductance greater than 8 pS and an obviously sigmoidal *g-V* relationship were included in our analysis. Data acquisition was performed using Axograph X software (Axograph, Canberra, Australia), whereas data analysis and graphical displays were accomplished using IGOR Pro software (IGOR Pro, Lake Oswego, OR). All experiments were performed at 32°C–34°C, and all data points are displayed as mean ± SEM.

Computer Simulations

Simulations were performed using the NEURON simulation environment (Carnevale and Hines, 2006) using morphologically precise CA1 pyramidal neuron reconstructions from the Duke-Southampton archive (http://neuron.duke.edu/cells/).

SUPPLEMENTAL INFORMATION

Supplemental Information for this article includes eight figures and Supplemental Experimental Procedures and can be found with this article online at doi:10.1016/j.neuron.2010.11.033.

ACKNOWLEDGMENTS

The authors thank members of the Center for Learning and Memory for helpful discussions and comments on the manuscript. The International Human Frontier Science Program Organization (R.N.) and the National Institutes of Health (fellowship to K.J.D.: MH90665; grants to D.J.: MH48432, MH44754, and NS37444) supported this study.

Accepted: September 23, 2010
Published: December 8, 2010

REFERENCES

Arnsten, A.F. (2009). Stress signalling pathways that impair prefrontal cortex structure and function. Nat. Rev. Neurosci. *10*, 410–422.

Baba, A., Yasui, T., Fujisawa, S., Yamada, R.X., Yamada, M.K., Nishiyama, N., Matsuki, N., and Ikegaya, Y. (2003). Activity-evoked capacitative Ca^{2+} entry: Implications in synaptic plasticity. J. Neurosci. *23*, 7737–7741.

Beck, H., and Yaari, Y. (2008). Plasticity of intrinsic neuronal properties in CNS disorders. Nat. Rev. Neurosci. *9*, 357–369.

Berridge, M.J. (2002). The endoplasmic reticulum: A multifunctional signaling organelle. Cell Calcium *32*, 235–249.

Biel, M., Wahl-Schott, C., Michalakis, S., and Zong, X. (2009). Hyperpolarization-activated cation channels: From genes to function. Physiol. Rev. *89*, 847–885.

Bojarski, L., Herms, J., and Kuznicki, J. (2008). Calcium dysregulation in Alzheimer's disease. Neurochem. Int. *52*, 621–633.

Bootman, M.D., Collins, T.J., Mackenzie, L., Roderick, H.L., Berridge, M.J., and Peppiatt, C.M. (2002). 2-aminoethoxydiphenyl borate (2-APB) is a reliable blocker of store-operated Ca^{2+} entry but an inconsistent inhibitor of InsP3-induced Ca^{2+} release. FASEB J. *16*, 1145–1150.

Brager, D.H., and Johnston, D. (2007). Plasticity of intrinsic excitability during long-term depression is mediated through mGluR-dependent changes in I_h in hippocampal CA1 pyramidal neurons. J. Neurosci. *27*, 13926–13937.

Cahalan, M.D. (2009). STIMulating store-operated Ca^{2+} entry. Nat. Cell Biol. *11*, 669–677.

Carnevale, N.T., and Hines, M.L. (2006). The NEURON Book (Oxford: Cambridge University Press).

Chang, F., Cohen, I.S., DiFrancesco, D., Rosen, M.R., and Tromba, C. (1991). Effects of protein kinase inhibitors on canine Purkinje fibre pacemaker depolarization and the pacemaker current I_f. J. Physiol. *440*, 367–384.

Chen, K., Aradi, I., Thon, N., Eghbal-Ahmadi, M., Baram, T.Z., and Soltesz, I. (2001). Persistently modified h-channels after complex febrile seizures convert the seizure-induced enhancement of inhibition to hyperexcitability. Nat. Med. *7*, 331–337.

Demaurex, N., Lew, D.P., and Krause, K.H. (1992). Cyclopiazonic acid depletes intracellular Ca^{2+} stores and activates an influx pathway for divalent cations in HL-60 cells. J. Biol. Chem. *267*, 2318–2324.

Fan, Y., Fricker, D., Brager, D.H., Chen, X., Lu, H.C., Chitwood, R.A., and Johnston, D. (2005). Activity-dependent decrease of excitability in rat hippocampal neurons through increases in I_h. Nat. Neurosci. *8*, 1542–1551.

Fan, Y., Deng, P., Wang, Y.C., Lu, H.C., Xu, Z.C., and Schulz, P.E. (2008). Transient cerebral ischemia increases CA1 pyramidal neuron excitability. Exp. Neurol. *212*, 415–421.

Frère, S.G., Kuisle, M., and Lüthi, A. (2004). Regulation of recombinant and native hyperpolarization-activated cation channels. Mol. Neurobiol. *30*, 279–305.

Frick, A., Magee, J., and Johnston, D. (2004). LTP is accompanied by an enhanced local excitability of pyramidal neuron dendrites. Nat. Neurosci. *7*, 126–135.

Jung, S., Jones, T.D., Lugo, J.N., Jr., Sheerin, A.H., Miller, J.W., D'Ambrosio, R., Anderson, A.E., and Poolos, N.P. (2007). Progressive dendritic HCN channelopathy during epileptogenesis in the rat pilocarpine model of epilepsy. J. Neurosci. *27*, 13012–13021.

Klejman, M.E., Gruszczynska-Biegala, J., Skibinska-Kijek, A., Wisniewska, M.B., Misztal, K., Blazejczyk, M., Bojarski, L., and Kuznicki, J. (2009). Expression of STIM1 in brain and puncta-like co-localization of STIM1 and ORAI1 upon depletion of Ca^{2+} store in neurons. Neurochem. Int. *54*, 49–55.

Lefkimmiatis, K., Srikanthan, M., Maiellaro, I., Moyer, M.P., Curci, S., and Hofer, A.M. (2009). Store-operated cyclic AMP signalling mediated by STIM1. Nat. Cell Biol. *11*, 433–442.

Lewis, A.S., Schwartz, E., Chan, C.S., Noam, Y., Shin, M., Wadman, W.J., Surmeier, D.J., Baram, T.Z., Macdonald, R.L., and Chetkovich, D.M. (2009). Alternatively spliced isoforms of TRIP8b differentially control h channel trafficking and function. J. Neurosci. *29*, 6250–6265.

Luik, R.M., Wang, B., Prakriya, M., Wu, M.M., and Lewis, R.S. (2008). Oligomerization of STIM1 couples ER calcium depletion to CRAC channel activation. Nature *454*, 538–542.

Lytton, J., Westlin, M., and Hanley, M.R. (1991). Thapsigargin inhibits the sarcoplasmic or endoplasmic reticulum Ca-ATPase family of calcium pumps. J. Biol. Chem. *266*, 17067–17071.

Magee, J.C. (1998). Dendritic hyperpolarization-activated currents modify the integrative properties of hippocampal CA1 pyramidal neurons. J. Neurosci. *18*, 7613–7624.

Marciniak, S.J., and Ron, D. (2006). Endoplasmic reticulum stress signaling in disease. Physiol. Rev. *86*, 1133–1149.

Mattson, M.P., LaFerla, F.M., Chan, S.L., Leissring, M.A., Shepel, P.N., and Geiger, J.D. (2000). Calcium signaling in the ER: Its role in neuronal plasticity and neurodegenerative disorders. Trends Neurosci. *23*, 222–229.

McDermott, C.M., LaHoste, G.J., Chen, C., Musto, A., Bazan, N.G., and Magee, J.C. (2003). Sleep deprivation causes behavioral, synaptic, and membrane excitability alterations in hippocampal neurons. J. Neurosci. *23*, 9687–9695.

Narayanan, R., and Johnston, D. (2007). Long-term potentiation in rat hippocampal neurons is accompanied by spatially widespread changes in intrinsic oscillatory dynamics and excitability. Neuron *56*, 1061–1075.

Narayanan, R., and Johnston, D. (2008). The h channel mediates location dependence and plasticity of intrinsic phase response in rat hippocampal neurons. J. Neurosci. *28*, 5846–5860.

Nicolay, N.H., Hertle, D., Boehmerle, W., Heidrich, F.M., Yeckel, M., and Ehrlich, B.E. (2007). Inositol 1,4,5 trisphosphate receptor and chromogranin B are concentrated in different regions of the hippocampus. J. Neurosci. Res. *85*, 2026–2036.

Nishiyama, M., Hong, K., Mikoshiba, K., Poo, M.M., and Kato, K. (2000). Calcium stores regulate the polarity and input specificity of synaptic modification. Nature *408*, 584–588.

Parekh, A.B., and Putney, J.W., Jr. (2005). Store-operated calcium channels. Physiol. Rev. *85*, 757–810.

Park, M.K., Choi, Y.M., Kang, Y.K., and Petersen, O.H. (2008). The endoplasmic reticulum as an integrator of multiple dendritic events. Neuroscientist *14*, 68–77.

Paschen, W., and Mengesdorf, T. (2005). Endoplasmic reticulum stress response and neurodegeneration. Cell Calcium *38*, 409–415.

Sankar, R., Shin, D.H., Liu, H., Mazarati, A., Pereira de Vasconcelos, A., and Wasterlain, C.G. (1998). Patterns of status epilepticus-induced neuronal injury during development and long-term consequences. J. Neurosci. *18*, 8382–8393.

Santoro, B., Piskorowski, R.A., Pian, P., Hu, L., Liu, H., and Siegelbaum, S.A. (2009). TRIP8b splice variants form a family of auxiliary subunits that regulate gating and trafficking of HCN channels in the brain. Neuron *62*, 802–813.

Seidler, N.W., Jona, I., Vegh, M., and Martonosi, A. (1989). Cyclopiazonic acid is a specific inhibitor of the Ca^{2+}-ATPase of sarcoplasmic reticulum. J. Biol. Chem. *264*, 17816–17823.

Shin, M., Brager, D., Jaramillo, T.C., Johnston, D., and Chetkovich, D.M. (2008). Mislocalization of h channel subunits underlies h channelopathy in temporal lobe epilepsy. Neurobiol. Dis. *32*, 26–36.

Thastrup, O., Cullen, P.J., Drøbak, B.K., Hanley, M.R., and Dawson, A.P. (1990). Thapsigargin, a tumor promoter, discharges intracellular Ca^{2+} stores by specific inhibition of the endoplasmic reticulum Ca^{2+}-ATPase. Proc. Natl. Acad. Sci. USA *87*, 2466–2470.

Uyama, Y., Imaizumi, Y., and Watanabe, M. (1992). Effects of cyclopiazonic acid, a novel Ca^{2+}-ATPase inhibitor, on contractile responses in skinned ileal smooth muscle. Br. J. Pharmacol. *106*, 208–214.

Vargas, G., and Lucero, M.T. (2002). Modulation by PKA of the hyperpolarization-activated current I_h in cultured rat olfactory receptor neurons. J. Membr. Biol. *188*, 115–125.

Verkhratsky, A. (2005). Physiology and pathophysiology of the calcium store in the endoplasmic reticulum of neurons. Physiol. Rev. *85*, 201–279.

Wang, Z., Xu, N.L., Wu, C.P., Duan, S., and Poo, M.M. (2003). Bidirectional changes in spatial dendritic integration accompanying long-term synaptic modifications. Neuron *37*, 463–472.

Woodard, G.E., López, J.J., Jardín, I., Salido, G.M., and Rosado, J.A. (2010). TRPC3 regulates agonist-stimulated Ca^{2+} mobilization by mediating the interaction between type I inositol 1,4,5-trisphosphate receptor, RACK1, and Orai1. J. Biol. Chem. *285*, 8045–8053.

Xu, C., Bailly-Maitre, B., and Reed, J.C. (2005). Endoplasmic reticulum stress: Cell life and death decisions. J. Clin. Invest. *115*, 2656–2664.

Yang, R.H., Wang, W.T., Hou, X.H., Hu, S.J., and Chen, J.Y. (2010). Ionic mechanisms of the effects of sleep deprivation on excitability in hippocampal pyramidal neurons. Brain Res. *1343*, 135–142.

Zhang, W., and Linden, D.J. (2003). The other side of the engram: Experience-driven changes in neuronal intrinsic excitability. Nat. Rev. Neurosci. *4*, 885–900.